Polymer Testing 115 (2022) 107759

Contents lists available at ScienceDirect

Polymer Testing

journal homepage: www.elsevier.com/locate/polytest

Developing a method for evaluating color changeover in a hot-runner multi-cavity injection mold

Dániel Török [a,b], Tatyana Ageyeva [a,b], Róbert Boros [a], Ágnes Kovács [c,d], József Gábor Kovács [a,b,*]

[a] Department of Polymer Engineering, Faculty of Mechanical Engineering, Budapest University of Technology and Economics, Műegyetem rkp. 3., H-1111, Budapest, Hungary
[b] MTA-BME Lendület Lightweight Polymer Composites Research Group, Műegyetem rkp. 3., H-1111, Budapest, Hungary
[c] Department of Biostatistics, University of Veterinary Medicine Budapest, István utca 2, H-1078, Budapest, Hungary
[d] Department of Applied Analysis and Computational Mathematics, Eötvös Loránd University, Pázmány Péter sétány 1/C, H-1117, Budapest, Hungary

ARTICLE INFO

Keywords:
Injection molding
Color changeover
Quality control
Multi-cavity mold

ABSTRACT

Quality control, which nowadays almost always involves the integration of online measurement methods into the production process, is of paramount importance for injection molding. Online pressure and temperature measurement is already widespread and essential for quality and production control. On the other hand, monitoring the appearance, color, or surface defects of products is less common. It is usually carried out with a camera system installed on a conveyor belt independently of the injection molding process. However, color defects in injection molded products, which are caused by the poor distribution of the colorant, are common defects that usually occur after color changeover in injection molding. Color changeover is currently not a well-controlled procedure, and it is associated with high additional costs. It also requires a large amount of material and causes extended downtime of the injection molding equipment. Color changeover can be even more complicated due to the specific design of the injection unit, the presence of static or dynamic mixers, and the hot runner system design of the molds. In this study, we develop a measurement method to monitor color change and the amount of material and time needed to clean the injection system. This method is based on digital image processing. It can be very useful in the plastic industry and can greatly help manufacturers to develop and produce more efficient injection molding systems.

1. Introduction

Injection molding is the most widely used and the most productive polymer processing technology—more than one-third of polymer products are injection molded [1,2]. To stay competitive, injection molding manufacturers need to produce parts that satisfy the increasing number of stringent quality requirements [3]. The quality of an injection molded part is a collective term that includes dimensional accuracy, mechanical properties, and appearance [4,5]. Although most research focuses on mechanical performance and dimensional accuracy, the appearance of injection-molded parts plays an even more important role in the market [6]. Surface defects worsen the appearance of an injection-molded part, which might result in the product becoming scrap. One of the critical surface defects is color inhomogeneity, which is usually caused by the improper mixing and bad dispersion of a colorant in the plastic [7] or by a color changeover.

A color changeover operation requires proper cleaning and the removal of the residual material from the injection molding system. Otherwise, non-uniform color distribution and even the degradation of the polymer can occur. At the same time, the cleaning of an injection unit and a mold with hot runners can take several hours. Although it is possible to replace polymer A with polymer B by purging the injection unit and the hot runner system together or separately (Fig. 1), it is difficult to determine the exact time of the process. This issue becomes even more complicated when a multi-cavity mold is used, due to the inherent imbalance of the runner system.

Another problem is that the inspection of the color or color homogeneity of an injection molded part is not automated in most cases and relies heavily on the human factor. The main issues of color inspection performed by an operator are an inevitable subjectivity and limited

* Corresponding author. Department of Polymer Engineering, Faculty of Mechanical Engineering, Budapest University of Technology and Economics, Műegyetem rkp. 3., H-1111, Budapest, Hungary.
E-mail address: kovacs@pt.bme.hu (J.G. Kovács).

https://doi.org/10.1016/j.polymertesting.2022.107759
Received 9 June 2022; Received in revised form 11 July 2022; Accepted 27 August 2022
Available online 31 August 2022

precision of the evaluation, and possible operator faults that can lead to loss of time and material. According to Liu et al. [8], the probability of scrap in injection molding can reach 2%, which is a considerable amount in mass production. Therefore, automation of color inspection can bring significant economic benefits to the manufacturers of injection molded parts.

To satisfy the requirements of Industry 4.0, the injection molding process needs to be fully automated and controlled [9,10]. According to Chen and Turng [11], full control of the injection molding process involves three levels: controlling machine parameters, in-mold parameters, and part quality. By now, controlling the machine and in-mold parameters has been well automated with the help of numerous sensors in different parts of the machines and molds [12]. By contrast, the control, and thus automation of the quality of injection molded parts, especially the color or color homogeneity of the part, is almost missing and highly depends on the operator's experience. The main reason for this is the absence of color sensors [13].

The solution for the automation of color measurement is digital imaging and digital image processing (DIP). Digital imaging by camera offers the non-contact acquisition of images of the parts produced. The analysis of the captured images helps to characterize color quality qualitatively and quantitively [14]. DIP technology is now widely used in many areas, such as metalwork [15], agriculture [16], the food industry [17], nuclear forensics [18] and fuel science [19]. In contrast, in the polymer industry, it is less common. Fleischer et al. [20] used DIP and a transparent injection mold to monitor the front position and distribution of fibers during injection molding. The authors offered this method as a part of a quality control system for the production of composite parts. In the studies of Jo et al. [21] and Janowski et al. [22], DIP is used to characterize fiber orientation in injection-molded products. Chen et al. [4] used DIP to monitor and measure shrinkage and the flash defects on the outer contour of injection-molded lenses. Amodio et al. [23] describe the use of DIP to control the appearance of injection-molded parts. They determined the intensity and uniformity of color by DIP and then detected small black dots on the surface of the parts produced. Zsíros et al. [6] developed a method to measure color inhomogeneity on injection molded parts by DIP and measured the influence of different injection molding processing parameters on color inhomogeneity. In another paper, Zsíros at al [24]. calibrated the proposed method with different colors and measured the differences between the homogenization properties of nine different masterbatch recipes.

Although particular progress has been achieved in evaluating color inhomogeneity, the problem of determining the time of color changeover in injection molding is still not solved. In this study, we show our method, which combines a quantitative evaluation of the color of the parts produced and helps calculate the time of color change. The proposed method has the following benefits: it (1) reduces the time for the color changeover, which is downtime for the injection molding machine; (2) it reduces the amount of scrap; (3) it characterizes mold imbalance and helps optimize the design of the runner system; (4) and it acquires data about part quality which are necessary for intelligent injection molding. The proposed method can be a part of an online system that monitors the quality of injection-molded parts.

2. Materials and methods

2.1. Equipment

2.1.1. An injection molding machine and a mold

We used an Arburg Allrounder 470 A 1000-290 injection molding machine (Arburg Holding GmbH, Lossburg, Germany) to produce samples and conduct the tests. The injection molding machine has a three-zone, universally designed core-progressive screw with a diameter of 30 mm, which is equipped with an Arburg screw tip. We used a hot runner two-cavity mold to produce discs with a diameter of 100 mm and a thickness of 2 mm. The nozzles of the hot runner system are pneumatically controlled needle valves (Fig. 2).

2.1.2. Equipment for image acquisition

Raw images were captured with an Epson Photo V600 flatbed scanner with a 300 dpi resolution. The images were 24-bit RGB colored. We did not use any corrections of the color or the histogram, nor did we use any smoothing or edge enhancement. The.bmp files were evaluated with the method we developed.

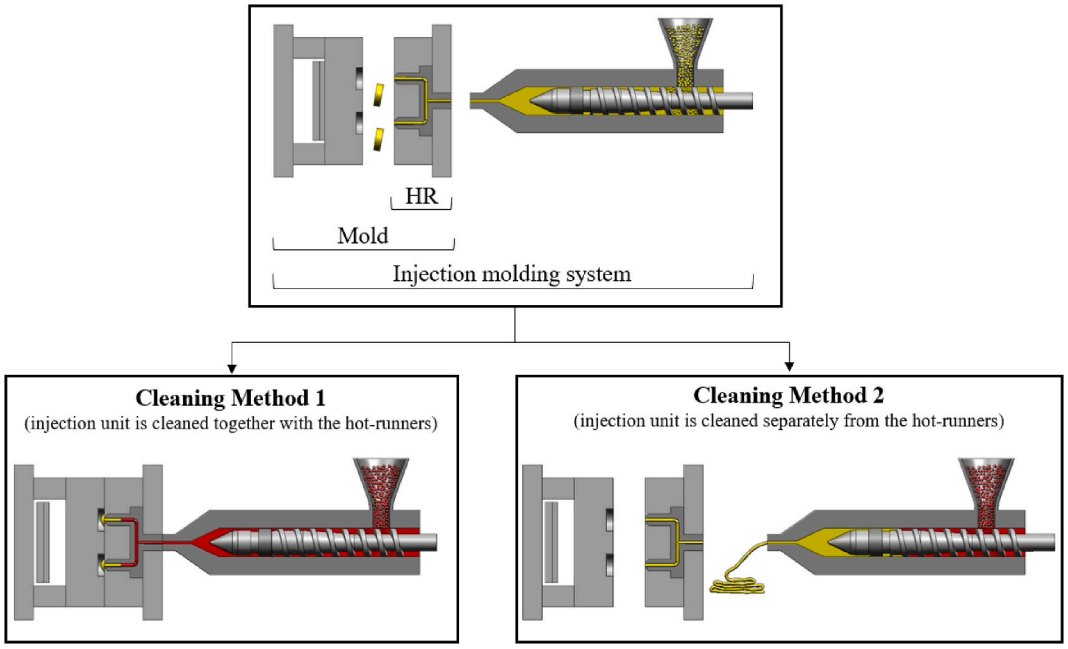

Fig. 1. Two ways of changing the color in injection molding (HR – hot runners). (For interpretation of the references to color in this figure legend, the reader is referred to the Web version of this article.)

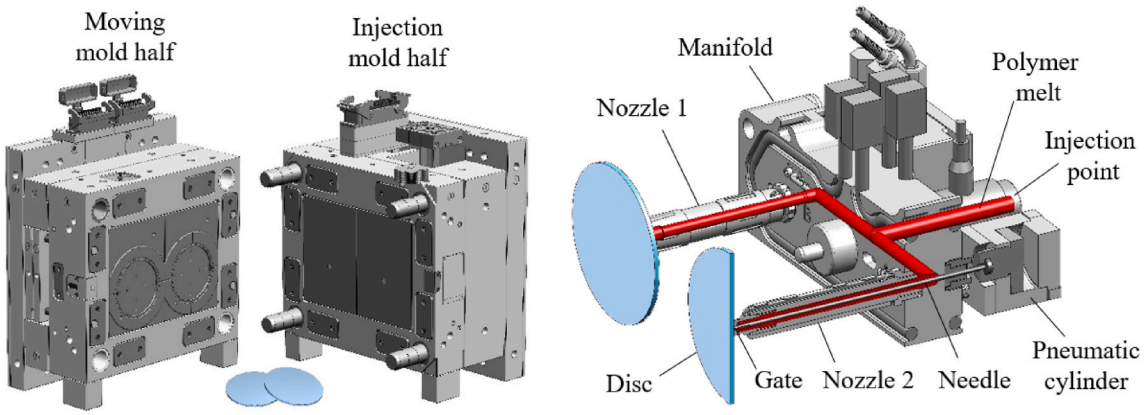

Fig. 2. The design of the two-cavity injection mold with the hot runner system.

2.2. Materials and the production of samples

We used ABS Terluran GP-35 NR (INEOS Styrolution, Frankfurt am Main, Germany; Melt Volume Rate is 34 cm^3/10 min at 220 °C/10 kg) for the color changeover test—uncolored (neat) ABS and colored ABS. The colored ABS consisted of 96 wt% neat ABS and 4 wt% blue-colored masterbatch (A. Schulman, Houston, Texas). Before the testing, both materials were dried according to the producer's recommendations (Table 1).

We first produced the blue-colored specimens. The processing parameters of injection molding are listed in Table 2. When stable production was achieved, homogeneous blue-colored parts were produced for five more cycles. After that, we initiated the cleaning process of the injection system. We used two different methods to clean the system (Fig. 1). In Case 1 the injection unit and the hot runner system were cleaned together, while in Case 2 we cleaned the injection unit separately from the hot runner system.

2.3. Cleaning tests

Case 1. After we reached stable production with the colored material, we stopped the process and removed the residual material from the hopper. Then, we filled the hopper with uncolored ABS and proceeded with production and collected the test samples for each cycle and each cavity individually for later identification. The production of test specimens continued until the cleaning process was completed. The end of the cleaning process was first determined by visual inspection. The cleaning of the injection unit and the hot runner system finished at approximately 135 cycles.

Case 2. This test aimed to clean the hot runner system separately from the injection unit. Therefore the injection unit had already been cleaned at the beginning of the test. When production with the colored ABS was finished, the injection unit was moved to its rear position, and the residual material was fully purged from the injection unit. After that, we filled the hopper with uncolored ABS. During the purging of the material from the injection unit, the material in the hot runner remained intact. After cleaning the injection unit, we continued production using the uncolored material for the hot runner test. The end of the cleaning process was also determined by visual inspection, and in this case, the total number of cycles was 105.

Table 1
Properties of the material used.

Property	Value
Drying temperature and time	80 °C for 4 h
Recommended melt temperature range	220–280 °C
Recommended mold temperature range	30–60 °C

Table 2
Processing parameters of injection molding.

Parameter	Value
Injection volume, cm^3	41
Injection speed, cm^3/s	40
Holding pressure, bar	700
Residual cooling time, s	7
Holding time, s	8
Clamping force, kN	1000
Screw rotation speed, m/min	25
Melt temperature, °C	245
Mold temperature, °C	70
Hot runner nozzle temperature, °C	230

2.4. Image acquisition, segmentation, and histogram data acquisition

For the analysis of the cleaning process in both cases described above, we produced a digital image for every sample with the flatbed scanner. We used the name of the scanned images to indicate in which cavity and in which cycle the specimen was made and the measurement series to which it belonged. This allowed an automated evaluation of the digital images later on. The schematic representation of the measurement layout is presented in Fig. 3. The digital images of the specimens at different cleaning states are shown in Fig. 4.

The first step of processing a digital image was segmentation, or in other words, the separation of the test objects from the background. We converted the images from the Red-Green-Blue (RGB) color space to the Hue-Saturation-Value (HSV) system for background separation. We did this transformation as the background can be distinguished easily based on the saturation value in the HSV color space. It was less than 5%, and this way it provided a simple threshold level for separation. After segmentation, the selected parts of the images (foreground) were converted to grayscale for further analysis. In Fig. 5, image segmentation and color conversion are shown.

The input to the further analysis of the cleaning process is a histogram of the grayscale images, showing the frequency of pixels corresponding to a given grayscale value. We obtained the relative frequency histograms by dividing the number of pixels in each class of a grayscale value by the number of pixels in the sample (Fig. 6).

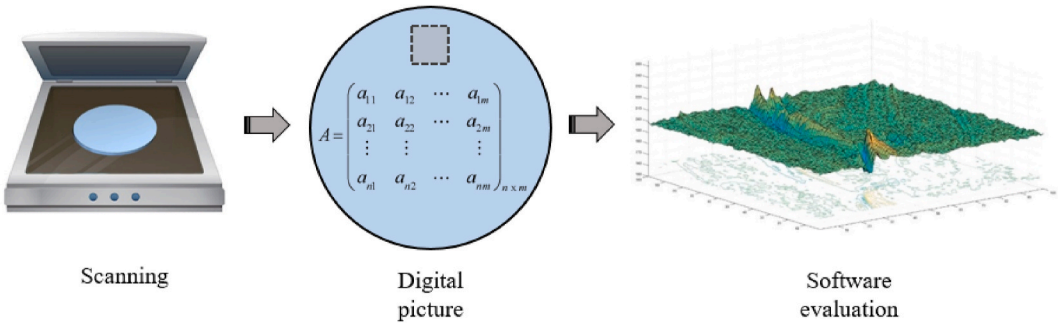

Fig. 3. The schematics of the measurement layout.

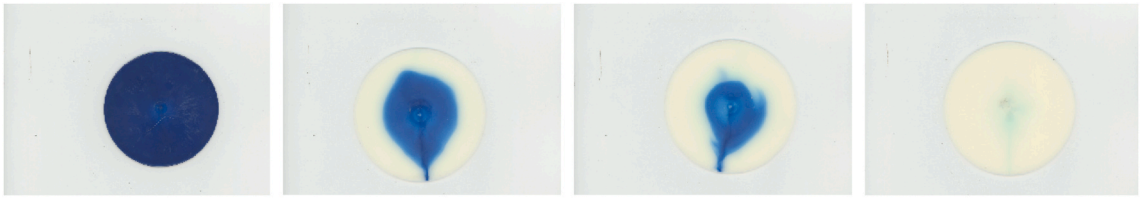

Fig. 4. The digital images of specimens: (a) cycle 1; (b) cycle 2; (c) cycle 5; (d) cycle 20 (for the Case 2).

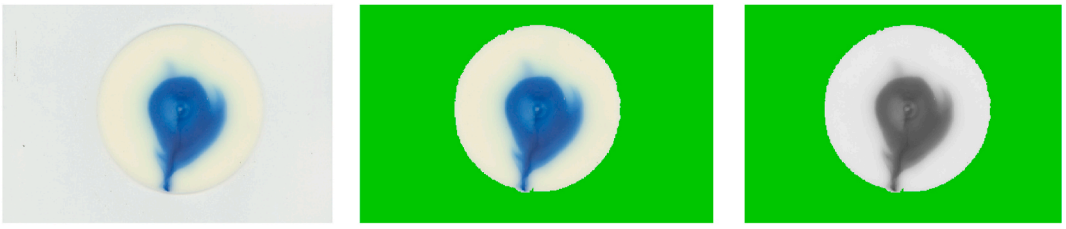

Fig. 5. The example of segmentation and color conversion: (a) an original image: (b) a segmented image; (c) a segmented grayscale image. (For interpretation of the references to color in this figure legend, the reader is referred to the Web version of this article.)

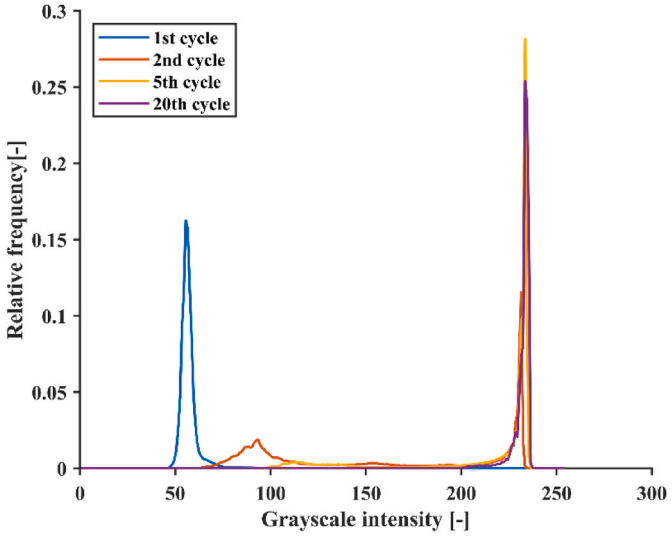

Fig. 6. An example of a relative frequency histograms for different test specimens (produced at Cycles 1, 2, 5, and 20).

3. Results and discussion

3.1. Development of the method for the determination of the time of color changeover in injection molding

3.1.1. Characterization of the cleaning process with the estimated average color

The cleaning process can be characterized with the change in relative frequency histograms obtained for the specimens produced in successive cycles. The color of the specimens produced after changing the material in the injection molding system progressively, cycle-by-cycle, turns from blue to the color of neat ABS. The color changes in the specimens are reflected in a shift of the histogram from lower grayscale intensity to higher grayscale intensity. This shift can be expressed numerically with the expected value of the grayscale intensity (the average color), which can be calculated with the formula:

$$S_x = \frac{\sum_{k=1}^{n} x_k . y_k}{\sum_{k=1}^{n} y_k} \quad (1)$$

where S_x is the average color of the test sample (hereafter, it will be referred to as "expected value"), x_k is the grayscale intensity of the kth bin of the histogram, and y_k is the number of pixels in the kth bin.

The expected value of coloration in the samples produced during the first two cycles and the related histograms are presented in Fig. 7. The

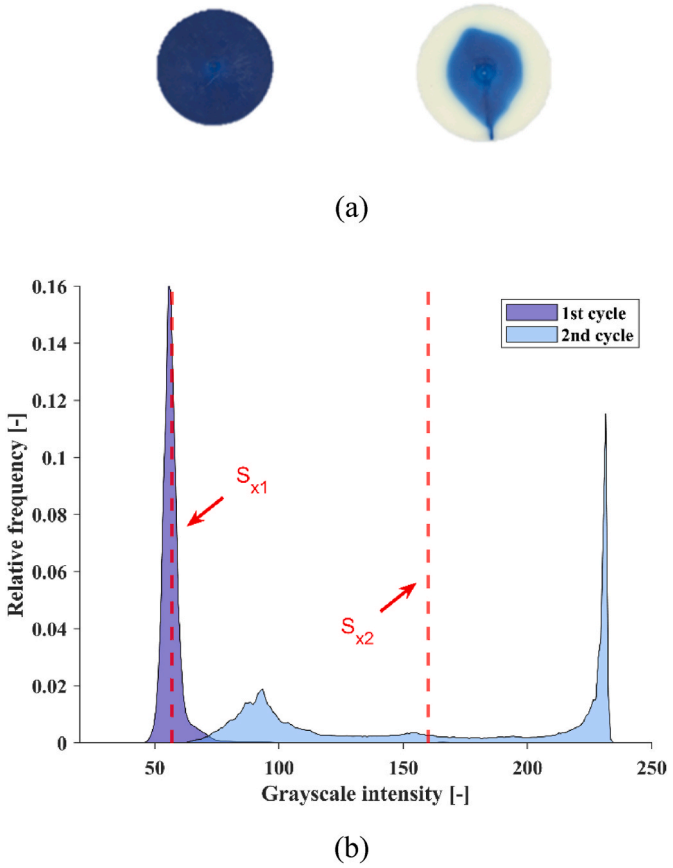

Fig. 7. The example of specimens produced in the first and second cycles (a) and their relative frequency histograms (b).

image of the test sample from the first cycle contained predominantly dark blue pixels, while the sample from the second cycle was dominated by white pixels. However, in the middle of the sample from the second cycle, a blue stain remained.

We calculated the expected value for all the specimens produced and plotted them as a function of cycle number (Fig. 8). With the progression of the number of cycles, the expected value (S_x) shifted towards a higher grayscale intensity. The expected value changed rapidly in the first ten cycles, which indicates that most of the blue-colored ABS left the system

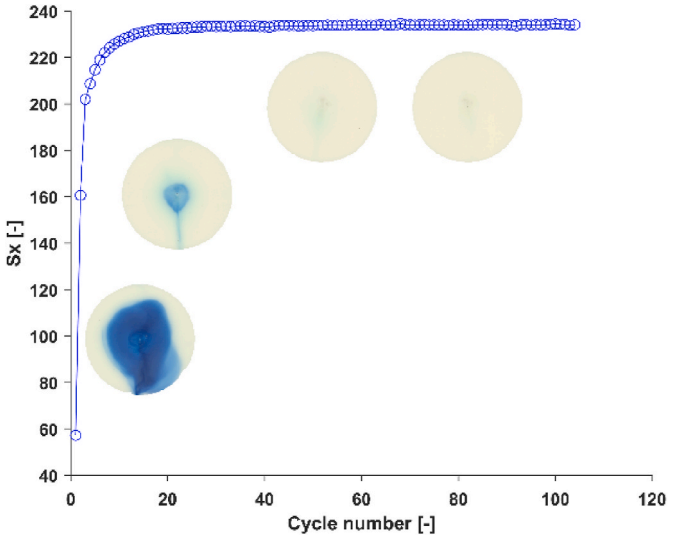

Fig. 8. The expected value as a function of cycle number.

during this period. After ten cycles, the cleaning process slowed down. This deceleration occurred because the melt flow in the injection unit and/or in the hot runners is not uniform, and therefore stagnant or slow-flowing sections may form. This slow phase of the cleaning process is not visible in the expected values curve (Fig. 8). However, this prolonged phase is essential as a defect-free product can only be produced when the blue-colored material leaves the system completely.

3.1.2. *Logarithmic scaling of the histogram*

The purpose of logarithmic scaling is to clearly highlight the differences between individual specimens during the prolonged, slow cleaning process (Fig. 9). Logarithmic scaling is more suitable for this purpose because it allows the histograms to clearly show a small number of impurities next to the majority of white pixels. In Fig. 9, the histograms of the samples from the first, second, tenth, and twentieth cycles are shown on a conventional (a) and a logarithmic scale (b). On the logarithmic curves, the 10th and 20th cycles are easily distinguishable, whereas, in the conventional histograms, only the 1st and 2nd cycles are visually different.

Similar to conventional histograms, the shift in the logarithmic curve can be expressed numerically by the expected value associated with the logarithmic curves (2).

$$Sx_{log} = \frac{\sum_{k=1}^{n} x_k \cdot \log(y_k)}{\sum_{k=1}^{n} \log(y_k)} \sqrt{b^2 - 4ac} \tag{2}$$

where $Sx_{\log}$ is the expected value of the logarithmic curve, x_k is the grayscale intensity of the kth bin of the histogram, and y_k is the number of pixels in the kth -bin.

The relationship between the $Sx_{\log}$ for the samples produced in the first two cycles and the logarithmic curves are illustrated in Fig. 10. The first test specimen contained predominantly dark blue pixels. However, a small number of light pixels are also visible on the logarithmic curve. This was not visible in the conventional histograms, as the number of blue pixels was several orders of magnitude greater than the number of light pixels.

The evolution of the expected value of the logarithmic curves as a function of cycle number is depicted in Fig. 11 (a). The comparison of the results with the regular grayscale intensity histograms and the logarithmic curves are presented in Fig. 11 (b). The use of the logarithmic curves has allowed us to separate the different cleaning stages better. In the first 3–4 cycles, the slope of the curve was steep and there was a rapid color shift, while in the next stage, up to the 25th cycle, cleaning was still steady but slower. In the last cleaning stage, the specimens were almost entirely the color of neat ABS, with only a small amount of color contamination still observed on their surfaces. In this last stage, some outliers appear ($Sx_{\log}$ value drops), presumably due to the washing out of stagnant particles that were stuck in the hot runner.

3.2. *Characterization of the cleaning process*

3.2.1. *Case 1 – the combined cleaning of a hot runner system and an injection unit*

The examination of the concurrent cleaning of the hot runner system and the injection unit allows us to better explore the cleaning process stages as the injection unit mixes old and new feedstock, which prolongs the cleaning process. The curve, which corresponds to the simultaneous cleaning of the injection unit and the hot runner system, is shown in Fig. 12, where the different stages of cleaning are distinguishable. In the first part of the cleaning curves, there is no change in the color of the test specimen for about the first two cycles. Here, a new feedstock is moving through the system continuously, cycle by cycle. The length of this stage is proportional to the volume of the barrel and the hot runner system. Over the subsequent 100 to 110 cycles, the color of the test specimens changes significantly (transition from dark to light). This section can be further split into two parts; the slope changes considerably around the

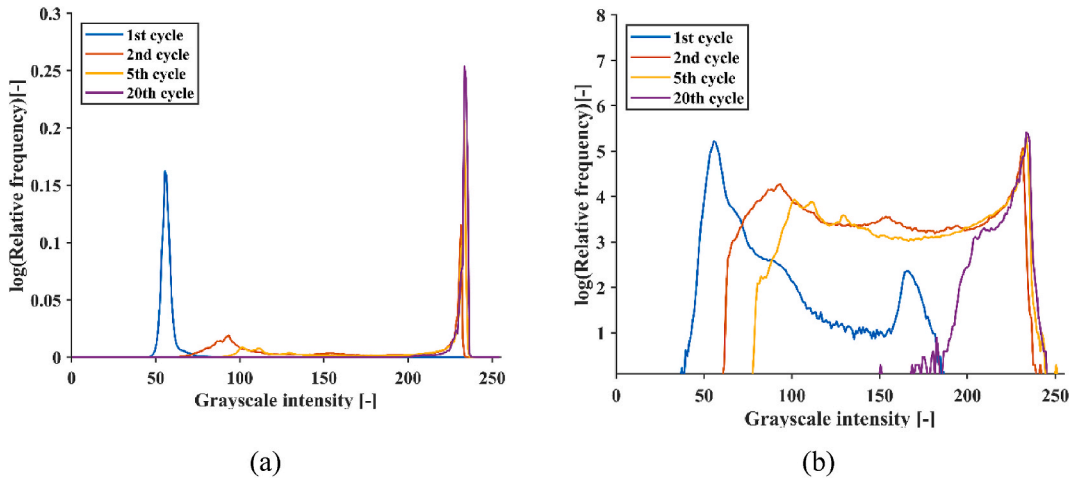

Fig. 9. The relative frequency histograms on a conventional scale (a) and on a 10-based logarithmic scale (b).

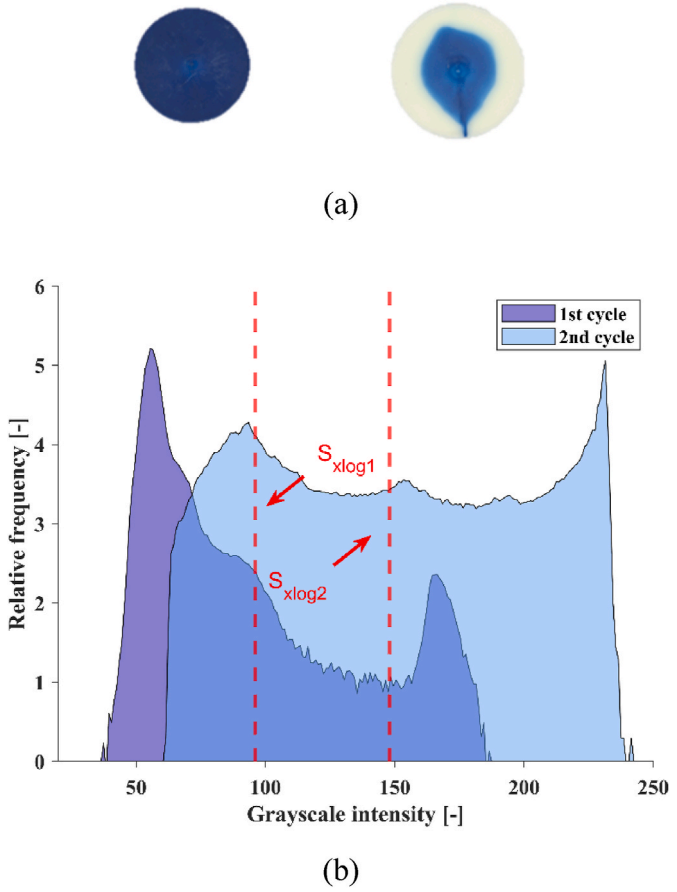

Fig. 10. The logarithmic curves of grayscale histograms and the expected values S_{xlog} (b) of the samples produced at the 1st and 2nd injection molding cycles (a).

20th cycle. It can be seen because the edge and the center part of the product becomes clean at different rates. The outer edge of the product cleans faster, while the center cleans more slowly. The stain in the middle of the sample and its slow cleaning may be due to the needle valve in the nozzle of the hot runner system. In this region, the flow of the polymer melt is not uniform, because the melt slows down along the wall of the needle valve (Fig. 2). After the 120th cycle, the system is considered clean, but small impurities may still be present in the product. However, the presence of small impurities does not change the overall color of a sample significantly.

3.2.2. *Case 2 – the separate cleaning of the hot runner system and injection unit*

Two branches can be distinguished in the hot runner system, which lead the polymer melt to the individual cavities. These branches are symmetrical to the centerline of the mold, so their cleaning should be almost identical. Fig. 13 shows the cleaning curve of the two nozzles of the hot runner. The first specimen is still the original blue color for both nozzles, and the color change starts only after this. The volume of material used in this cycle is about the same as the volume of the hot runner system. In the present case, the volume of channels is comparable with the volume of a product, so one cycle is sufficient for the new material to appear in the product. In the transition section of the cleaning curve, another break point can be observed around cycle 4. The break point indicates that the flow in the nozzles is not uniform, with both fast (away from the wall and needle valve) and slow (near the wall, around the needle valve) flow regions developing in the channel. These parts with different flow rates are cleaned at different rates. For both nozzles, after about the 24th cycle, the color of the test specimens no longer changes significantly, with only a few outliers observed. Based on the cleaning curves, there is no significant difference between the two branches of the hot runner system.

3.3. *Modeling of the cleaning process and comparison of the cleaning cases*

To numerically characterize the cleaning process, we fitted a model to the measured data. A saturation function with delay time was used to describe the cleaning curve of the hot runner. This function is not accurate in the early stages of the cleaning process, but it is accurate at the end of the process. If it is crucial to describe the early stages precisely, a more complex curve is needed. Practically, that is not necessary. The cleaning curve function we used is:

$$f(x) = 1 - e^{-(x-t)/\tau} \tag{3}$$

where x is the number of cycles, t is the delay time, and τ is the time constant of the saturation function. If the time constant is different, it shows that the cleaning rate of the branches is also different.

Case 1 *(combined cleaning)*. We fitted the model for both nozzles. The time delay was ten cycles for both nozzles and the time constants were 30 and 27 for Nozzle 1 and Nozzle 2, respectively. Our model also determines how many cycles are necessary for the cleaning curve to reach 99% saturation. It was 148 cycles for Nozzle 1 and 134 cycles for Nozzle

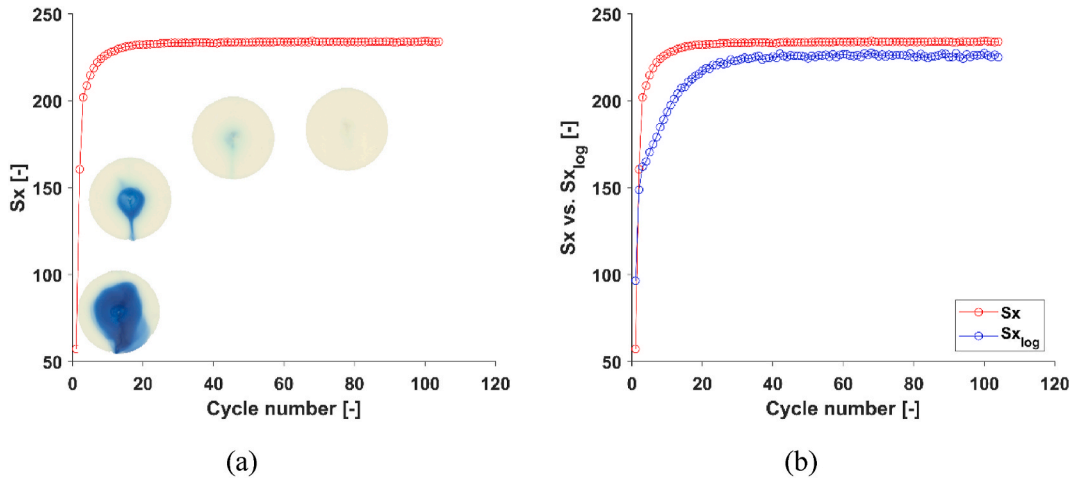

Fig. 11. The evolution of the expected values of the logarithmic curves of grayscale intensity as a function of cycle number (a) and the comparison of the results with expected values of the regular histograms (b).

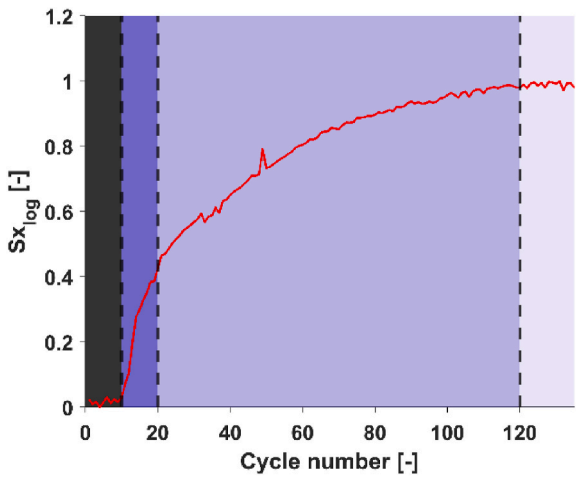

Fig. 12. The expected value of the logarithm of grayscale intensity as a function of the number of cycles when the injection unit and the hot runner system are cleaned simultaneously.

2 (Fig. 14). The cleaning process is slightly longer for Nozzle 1 than for Nozzle 2, so the whole cleaning process should be at least 148 cycles. As we know the number of cycles needed to clean the system, we can calculate the amount of material needed, using the injection volume and the density of ABS. The amount of material was 6.3 kg in Case 1, where we cleaned the injection unit and the hot runner system together.

Case 2 (sep*arate cleaning)*. For Case 2, when we cleaned the hot runner system independently, we used 1.7 kg of ABS to clean the injection unit before the cleaning process of the hot runner system. Then we evaluated our model and calculated the time delay for both nozzles of the hot runner system (Fig. 15). The time delay was one cycle for both nozzles and the time constants were 7.015 and 7.118 for the Nozzle 1 and Nozzle 2, respectively. The slight difference in the time constant and the number of cycles needed to reach the clean state suggest that the flows in the two branches are almost identical. We determined the number of cycles for 99% cleaning of the nozzles, which was 34 cycles for both nozzles. The amount of material necessary to clean the hot runner system independently was around 1.5 kg. The total amount of the material used in Case 2 was 3.2 kg, a little more than half of the material used in Case 1.

Therefore, we proved that the cleaning process is more efficient when the injection unit and the hot runner system are cleaned independently (Table 3).

4. Conclusion

We developed a measurement and evaluation method to monitor the color changeover during injection molding. With this method, the color

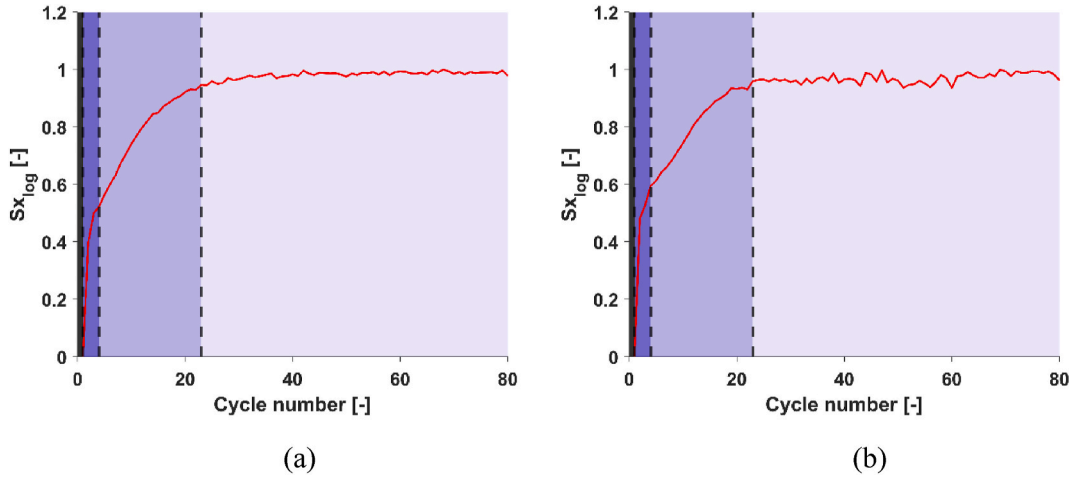

Fig. 13. The evolution of the expected value of the logarithm of the grayscale value as a function of the number of cycles: (a) for the Nozzle 1; (b) for the Nozzle 2.

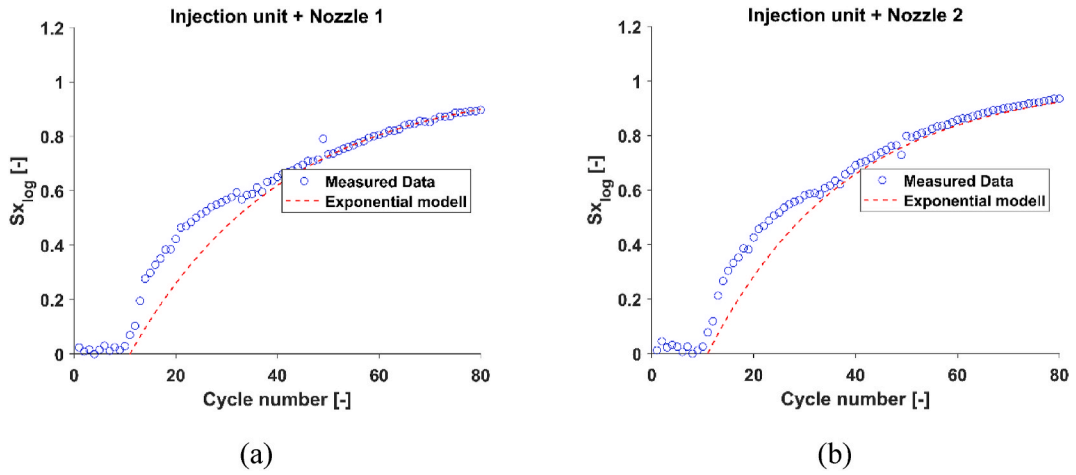

Fig. 14. The evolution of the expected value of the logarithmic curves as a function of cycle number and the fitted model for Case 1: (a) for the injection unit and Nozzle 1; (b) for the injection unit and Nozzle 2.

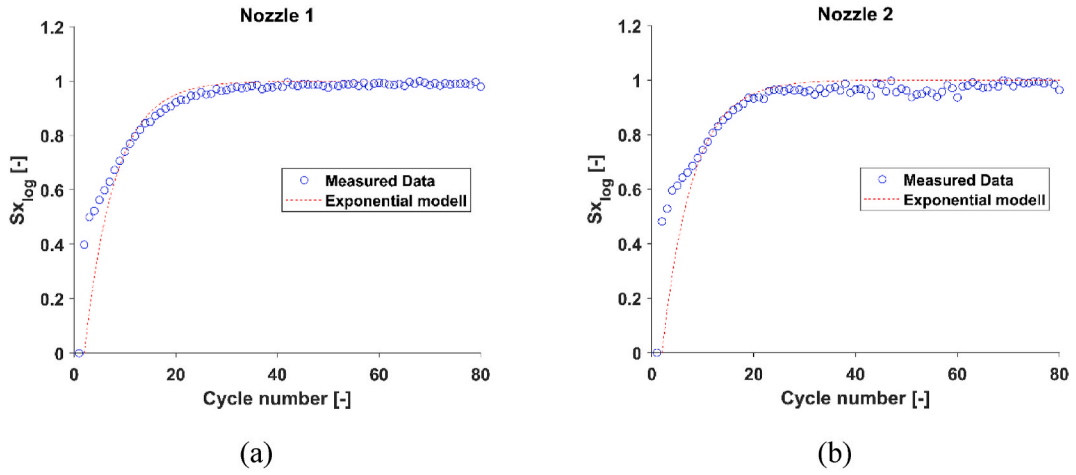

Fig. 15. The evolution of the expected value of the logarithmic curves as a function of cycle number and the fitted model for Case 2: (a) for Nozzle 1; (b) for Nozzle 2.

Table 3
Comparison of the cleaning characteristics for Case 1 and Case 2.

Characteristic	Case 1 (combined cleaning of the injection unit and hot runners)		Case 2 (separate cleaning of the injection unit and hot runners)	
	Nozzle 1	Nozzle 2	Nozzle 1	Nozzle 2
Time constant	~30	~27	7015	7118
Number of cycles until the system is 99% clean	148	132	34	34
The total amount of material necessary for cleaning	6,3 kg		3,2 kg	

changeover procedure can be planned and thus become more efficient. Understanding the color changeover process helps engineers to develop it further and optimize hot runner molds. We presented a measurement setup consisting of an injection molding machine, a hot runner mold, and an imaging system to verify the method. We have demonstrated that color changeover can be accurately and quantitatively described cycle by cycle. The main steps of the evaluation are the digitization of the product and the subsequent image analysis. As a first step, we automatically isolate the product in the image and then construct a histogram from the pixels associated with the product. From this, we calculate the expected value of the grayscale intensity of the pixels for each cycle. Using this evaluation method, we investigated the cleaning of a hot runner mold after color change. We found that the whole cleaning process can be investigated better with logarithmic curves of the histograms. In this case, the expected value was determined from the logarithmic curves. Plotting this as a function of cycle number, we found that the process during color change follows a saturation behavior and can be approximated well with a simple saturation curve with a time delay. The saturation curve we used required two fitting parameters, the time constant and the delay time, which described the color change process with 97.8% accuracy for our measured data points. With these two parameters, the cleaning of the injection unit and the hot runner systems of different designs can be well quantified and compared. Using the method, we found that cleaning is more efficient if the injection unit and the hot runner system are cleaned independently of each other (Case 2: 3.2 kg). In this case, the time and material consumption was 50% less than when we cleaned the injection unit and hot runners together (Case 1: 6.3 kg). In addition, we found that the measured hot runner system is well balanced, and the polymer melt flow is very similar in both nozzles, as the time constants are almost equal for both nozzles.

Funding

This work was supported by the National Research, Development and Innovation Office, Hungary (2019-1.1.1-PIACI-KFI-2019-00205,

2018-1.3.1-VKE-2018-00001, 2017-2.3.7-TÉT–IN–2017-00049). The research reported in this paper was supported by the BME NC TKP2020 grant of NKFIH Hungary. The research was done under the scope of the Project no. RRF-2.3.1-21-2022-00009, entitled "National Laboratory for Renewable Energy" which has been implemented with the support provided by the Recovery and Resilience Facility of the European Union within the framework of Programme Széchenyi Plan Plus.

CRediT authorship contribution statement

Dániel Török: Conceptualization, Methodology, Investigation, Visualization, Writing – original draft. **Tatyana Ageyeva:** Visualization, Writing – review & editing. **Róbert Boros:** Investigation, Visualization. **Ágnes Kovács:** Formal analysis, Formal analysis. **József Gábor Kovács:** Supervision, Conceptualization, Resources, Methodology, Funding acquisition.

Declaration of competing interest

The authors declare that they have no known competing financial interests or personal relationships that could have appeared to influence the work reported in this paper.

Acknowledgments

The authors thank Arburg Hungaria Kft for the Arburg Allrounder 470 A 1000-290 injection molding machine, AQ Anton Kft for manufacturing the mold, and Meusburger Georg GmbH & Co KG for the mold elements and the hot-runner system.

References

[1] Computer Modeling for Injection Molding: Simulation, Optimization, and Control, John Wiley & Sons, Inc., Hoboken, NJ, USA, 2013, https://doi.org/10.1002/9781118444887p416.

[2] J.F. Campuzano, I.D. López, Study of the effect of dicumyl peroxide on morphological and physical properties of foam injection molded poly(lactic acid)/poly(butylene succinate) blends, Express Polym. Lett. 14 (2020) 673–684, https://doi.org/10.3144/expresspolymlett.2020.55.

[3] M.Z. Huang, J. Nomai, A.K. Schlarb, The effect of different processing, injection molding (im) and fused deposition modeling (fdm), on the environmental stress cracking (esc) behavior of filled and unfilled polycarbonate (pc), Expreess Polymer Letters 15 (2021) 194–202, https://doi.org/10.3144/expresspolymlett.2021.18.

[4] Y. Yang, B. Yang, S. Zhu, X. Chen, Online quality optimization of the injection molding process viadigital image processing and model-free optimization, J. Mater. Process. Technol. 226 (2015) 85–98, https://doi.org/10.1016/j.matprotec.2015.07.001.

[5] T. Tábi, K. Pölöskei, The effect of processing parameters and calcium-stearate on the ejection process of injection molded poly(lactic acid) products, Period. Polytech. - Mech. Eng. 66 (2022) 17–25, https://doi.org/10.3311/PPme.18246.

[6] L. Zsíros, A. Suplicz, G. Romhány, J.G. Kovacs, Development of a novel color inhomogeneity test method for injection molded parts, Polym. Test. 37 (2014) 112–116, https://doi.org/10.1016/j.polymertesting.2014.05.009.

[7] L. Zsíros, D. Török, J.G. Kovács, The effect of masterbatch recipes on the homogenization properties of injection molded parts, Int. J. Poly. Sci. 2017 (2017) 7, https://doi.org/10.1155/2017/5745878.

[8] J. Liu, F. Guo, H. Gao, M. Li, Y. Zhang, H. Zhou, Defect detection of injection molding products on small datasets using transfer learning, J. Manuf. Process. 70 (2021) 400–413, https://doi.org/10.1016/j.jmapro.2021.08.034.

[9] Z. Wang, W. Feng, J. Ye, J. Yang, C. Liu, A study on intelligent manufacturing industrial internet for injection molding industry based on digital twin, Complexity 2021 (16) (2021), https://doi.org/10.1155/2021/8838914.

[10] H. Lee, K. Ryu, Y. Cho, A framework of a smart injection molding system based on real-time data, Procedia Manuf. 11 (2017) 1004–1011, https://doi.org/10.1016/j.promfg.2017.07.206.

[11] Z. Chen, L.-S. Turng, A review of current developments in process and quality control for injection molding, Adv. Polym. Technol. 24 (2005) 165–182, https://doi.org/10.1002/adv.20046.

[12] T. Ageyeva, S. Horváth, J.G. Kovács, In-mold sensors for injection molding: on the way to industry 4.0, Sensors 19 (2019) 3551, https://doi.org/10.3390/s19163551.

[13] P. Zhao, J. Zhang, Z. Dong, J. Hung, H. Zhou, J. Fu, L.-S. Turng, Intelligent injection molding on sensing, optimization, and control, Adv. Polym. Technol. 2020 (2020) 22, https://doi.org/10.1155/2020/7023616.

[14] D. Török, J.G. Kovács, Effects of dynamic mixers on the color homogeneity and the process in injection molding, Poluymer Eng. Sci. 59 (2019) E189–E195, https://doi.org/10.1002/pen.25026.

[15] M. Jurevicius, J. Skeivalas, R. Urbanavicius, Analysis of surface roughness parameters digital image identification, Measurements 56 (2014) 81–87, https://doi.org/10.1016/j.measurement.2014.06.005.

[16] G. Veerendra, R. Swaroop, D.S. Dattu, C. Aruna Jyothi, M.K. Singh, Detecting plant diseases, quantifying and classifying digital image processing techniques, Mater. Today Proc. 51 (1) (2021) 837–841, https://doi.org/10.1016/j.matpr.2021.06.271.

[17] J. Rahimi, J. Baur, A. Singh, Digital imaging as a tool to study the structure of porous baked foods, J. Cereal. Sci. 95 (2020), 103084, https://doi.org/10.1016/j.jcs.2020.103084.

[18] N.B.A. Thompson, S.E. O'Sullivan, R.J. Howell, D.J. Bailey, M.R. Gilbert, N. C. Hyatt, Objective colour analysis from digital images as a nuclear forensic tool, Forensic Sci. Int. 139 (2021), 110678, https://doi.org/10.1016/j.forsciint.2020.110678.

[19] M.R. Soosai, Y.C. Joshya, R.S. Kumar, I.G. Moorthy, S. Karthikumar, N.T.L. Chi, A. Pugazhendhi, Versatile image processing technique for fuel science: a review, Sci. Total Environ. 780 (2021), 146469, https://doi.org/10.1016/j.scitotenv.2021.146469.

[20] P. Moll, A. Schafer, S. Coutandin, J. Fleischer, Method for the investigation of mold filling in the fiber injection molding process based on image processing, in: F. Dietrich, N. Krenkel (Eds.), 7th CIRP Global Web Conference "Towards Shifted Production Value Stream Patterns through Inference of Data, Models, and Technology", 2019, https://doi.org/10.1016/j.procir.2020.01.012pp156-161. Procedia CIRP.

[21] E.G. Kim, J.K. Park, S.H. Jo, A study on fiber orientation during the injection molding of fiber-reinforced polymeric composites (comparison between image processing results and numerical simulation), J. Mater. Process. Technol. 111 (2001) 225–232, https://doi.org/10.1016/S0924-0136(01)00521-0.

[22] A. Bednarz, W. Frącz, G. Janowski, The use of image analysis in evaluation of the fibers orientation in wood-polymer composites (wpc), Open Eng. 6 (2016) 737–741, https://doi.org/10.1515/eng-2016-0099.

[23] M. Sasso, M. Natalini, D. Amodio, Digital image processing for quality control on injection molding products, in: O. Ivanov (Ed.), Application and Experiences of Quality Control, InTech, Rijeka, Croatia, 2011, pp. 555–578.

[24] L. Zsíros, D. Török, J.G. Kovács, Evaluation of the homogenization properties of masterbatches, Color. Technol. 133 (2017) 431–438, https://doi.org/10.1111/cote.12298.